

DMD#23119

***TITLE PAGE***

***Microdialysis Evaluation of Atomoxetine Brain Penetration and Central  
Nervous System Pharmacokinetics in Rats***

*William Kielbasa, J. Cory Kalvass, Robert Stratford*

*Lilly Research Laboratories, Indianapolis, IN 46285*

DMD#23119

***RUNNING TITLE PAGE***

***a) Running title: Atomoxetine Brain Disposition and CNS PK in Rats***

***b) Name: William Kielbasa; Phone: 317-277-2788; Fax: 317-277-6661***

***Email: [kielbasa\\_william@lilly.com](mailto:kielbasa_william@lilly.com)***

***c) Number of text pages: 31; Number of tables: 1; Number of figures: 5; Number of references: 17; Number of words in the Abstract: 232; Number of words in the Introduction: 603; Number of words in the Discussion: 1077***

***d) List of non-standard abbreviations. BBB, blood brain barrier; BCB, blood cerebrospinal fluid barrier; ECF, extracellular fluid; CSF, cerebrospinal fluid; CNS, central nervous system; PK, pharmacokinetics;  $C_B$ , whole brain concentration;  $C_{BC}$ , concentration associated with the brain cell;  $C_{uBC}$ , unbound concentration associated with the brain cell;  $C_P$ , steady-state plasma concentration;  $C_{uP}$ , steady-state plasma unbound concentration;  $C_{ECF}$ , steady-state brain ECF concentration;  $C_{CSF}$ , CSF concentration;  $CL$ , unbound plasma clearance;  $Q_{BCB}$ , distributional clearance at the BCB;  $Q_{BBB}$ , distributional clearance at the BBB;  $CL_{ECF-CSF}$ , clearance from the ECF to the CSF;  $CL_{ECF-BC}$ , clearance from the ECF to the brain cell;  $CL_{BC-ECF}$ , clearance from the brain cell to the ECF;  $V$ , unbound plasma volume of distribution;  $V_{ECF}$ , brain ECF volume;  $V_{BC}$ , brain cell volume;  $V_B$ , total brain volume;  $V_{CSF}$ , CSF volume.***

DMD#23119

## ABSTRACT

A comprehensive in vivo evaluation of brain penetrability and CNS pharmacokinetics (PK) of atomoxetine in rats was conducted using brain microdialysis. We sought to determine the nature and extent of transport at the blood brain barrier (BBB) and blood cerebrospinal fluid barrier (BCB) and to characterize brain extracellular and cellular disposition. The steady-state extracellular fluid to plasma unbound concentration ratio ( $C_{ECF}/C_{uP} = 0.7$ ) and the cerebrospinal fluid to plasma unbound concentration ratio ( $C_{CSF}/C_{uP} = 1.7$ ) were both near unity indicating that atomoxetine transport across the BBB and BCB are primarily passive. Based on the ratios of whole brain concentration to  $C_{ECF}$  ( $C_B/C_{ECF} = 170$ ), brain cell concentration to  $C_{ECF}$  ( $C_{BC}/C_{ECF} = 219$ ) and unbound brain cell concentration to  $C_{ECF}$  ( $C_{uBC}/C_{ECF} = 2.9$ ) we conclude that whole brain concentration does not represent the concentration in the biophase and atomoxetine primarily partitions into brain cells. The distributional clearance at the BBB ( $Q_{BBB} = 0.00110$  L/h) was estimated to be 12-times more rapid than at the BCB ( $Q_{BCB} = 0.0000909$  L/h) and similar to the clearances across brain parenchyma ( $CL_{ECF-BC} = 0.00216$  L/h;  $CL_{BC-ECF} = 0.000934$  L/h). In summary, the first detailed examination using a quantitative microdialysis technique to understand the brain disposition of atomoxetine was conducted. We determined that atomoxetine brain penetration is high, movement across the BBB and BCB occur predominantly by a passive mechanism and rapid equilibration of ECF and CSF with plasma occurs.

DMD#23119

## INTRODUCTION

Transport into the central nervous system (CNS) is essential for drugs that have pharmacological targets within the brain. The CNS exposure of a drug is determined by the blood-brain-barrier (BBB) and blood-cerebrospinal fluid-barrier (BCB) transport processes and the kinetics governing distribution and elimination. The CNS pharmacokinetics (PK) of a drug is an important determinant in the time course and intensity of effect. Non-homogeneous distribution within brain can occur due to physicochemical properties of a drug, cellular binding or the presence of active transporters at the neuronal cell membranes. Understanding brain distribution is important because it can provide valuable insights pertaining to the pharmacological actions of a drug.

It is generally accepted that only unbound drug in plasma crosses the BBB and interacts with receptors. Equilibration across the BBB and BCB can be expressed by the ratios  $C_{ECF}/C_{uP}$  and  $C_{CSF}/C_{uP}$ , respectively. When near unity is obtained from such ratios, distribution is consistent with transport by passive diffusion, or the impact of influx and efflux transport is equal. If a ratio below unity is obtained it is consistent with an active process limiting distribution such as BBB efflux, CSF bulk flow or metabolism, and a value above unity is consistent with an active influx process enhancing distribution. A ratio of  $\pm 3$ -fold was meaningful to assess the contribution of a passive mechanism at the BBB based on unbound plasma and brain fractions of drugs (Kalvass et al., 2007; Maurer et al., 2005). In addition, the brain to plasma ratios of Pgp knock-out and wild-type

DMD#23119

animals were investigated and a ratio of  $\pm 3$ -fold did not appear to have much impact on the success of drugs as CNS-active compounds (Doran et al., 2005).

Atomoxetine HCl (Strattera®, (-)-N-methyl-3-phenyl-3-(o-tolylloxy)-propylamine hydrochloride) has been developed as a therapeutic agent for the treatment of attention deficit/hyperactivity disorder (ADHD), a behavioral disorder characterized by inappropriate levels of motor activity, impulsivity, distractibility and inattention (Biederman, 2005; Biederman and Faraone, 2002). Atomoxetine inhibited binding of radioligands to clonal cell lines transfected with human norepinephrine (NE), serotonin (5-HT) and dopamine (DA) transporters with dissociation constant ( $K_i$ ) values of 5, 77 and 1451 nM, respectively, demonstrating selectivity for NE transporters. In rat brain microdialysis studies, atomoxetine increased ECF levels of NE and DA in the prefrontal cortex (PFC) similarly, but did not alter 5-HT levels, leading to the hypothesis that the atomoxetine-induced increase of catecholamines in the PFC, a region involved in attention and memory, may play a pivotal role in the therapeutic effects of atomoxetine in ADHD (Bymaster et al., 2002).

The atomoxetine ECF concentration at the NE transporter (NET), the site where atomoxetine inhibits NE re-uptake into the neuron, is key to atomoxetine pharmacological activity. The systemic PK of atomoxetine has been well described in animals and humans (Mattiuz et al., 2003; Sauer et al., 2005); however, limited data exist regarding the disposition in the CNS where the actions of atomoxetine arise. In vitro investigations showed that atomoxetine brain permeability in MDR1-MDCK cells and in situ brain permeability was relatively moderate compared to 49 other marketed drugs for CNS indications (Summerfield et al., 2007). The objective of the present study was to

DMD#23119

conduct a comprehensive *in vivo* evaluation of CNS penetrability and disposition of atomoxetine in rats. We sought to determine the nature and extent of transport at the BBB and BCB and to characterize brain extracellular and cellular disposition. Following steady-state infusions of atomoxetine, we collected ECF using brain microdialysis and estimated the brain extracellular and cellular concentrations of atomoxetine. Plasma, CSF and whole brain samples were also collected using conventional PK techniques and assayed for atomoxetine. A neuropharmacokinetic model was developed to characterize the CNS disposition of atomoxetine.

DMD#23119

## METHODS

**Drugs and Chemicals.** Atomoxetine HCl and its stable label,  $^2\text{H}_7$ -atomoxetine, were synthesized at Eli Lilly and Company. The dialysis buffer was prepared using reagent grade materials purchased from Sigma-Aldrich. The composition of the dialysis media (pH 7 – 7.5) was 1.3 mM  $\text{CaCl}_2$ , 1 mM  $\text{MgCl}_2$ , 3 mM KCl, 147 mM NaCl, 1 mM  $\text{Na}_2\text{HPO}_4 \times 7\text{H}_2\text{O}$ , 0.2 mM  $\text{NaH}_2\text{PO}_4 \times \text{H}_2\text{O}$  and was prepared in deionized water and filtered through a 0.22 micron filter. For retrodialysis calibration studies, dialysis buffer stock solutions containing 0.1 mg/mL atomoxetine HCl and  $^2\text{H}_7$ -atomoxetine were prepared and stored at  $-70^\circ\text{C}$ . One day prior to use, an aliquot of stock solution was diluted to 100 ng/ml with dialysis buffer and refrigerated. For PK studies, systemic infusion solutions of 5% dextrose in water (Braun Medical, Irvine, CA) containing 1 mg/mL atomoxetine HCl were prepared and stored at  $-70^\circ\text{C}$ . Stock solutions of dialysis buffer containing 0.1 mg/mL  $^2\text{H}_7$ -atomoxetine were also prepared and stored at  $-70^\circ\text{C}$ . One day prior to use, an aliquot of dialysis buffer stock solution was diluted to 100 ng/ml  $^2\text{H}_7$ -atomoxetine with dialysis buffer and the systemic infusion stock solution was removed from the freezer. Both solutions were refrigerated until use. Solvents used for HPLC analysis were of reagent grade (OmniSolv, EMD Chemicals, Gibbstown, NJ).

**Animal Preparation.** Male Sprague-Dawley rats weighing between 275 – 325 grams were surgically prepared at Charles River (Boston, MA) to support intravenous administration and arterial blood collection via femoral vein/artery cannulations. A BAS guide cannula (Bioanalytical Systems, West Lafayette, IN) was implanted in the medial-prefrontal cortex (coordinates: AP +3.2 mm, ML +0.6 mm and DV – 2.2 mm). Upon

DMD#23119

receipt, rats were acclimated for 3 days. One day before an experiment, a BAS-4 probe was inserted and perfused with dialysis buffer for 18-24 hours at a flow rate of 0.2  $\mu\text{L}/\text{min}$ . The live phase portion of a study was conducted on a Culex Automated Pharmacology System (Bioanalytical Systems) that enabled timed blood and dialysate collections in awake and freely moving animals. Animals were allowed free access to food and water during the time course of sample collection. All activities were performed humanely under a protocol approved by the Eli Lilly and Company Institutional Animal Care and Use Committee in an animal facility accredited by the Association for Assessment and Accreditation of Laboratory Animal Care, International.

**Evaluation of Plasma and Brain Binding.** The atomoxetine unbound plasma fraction ( $f_{\text{uP}}$ ) and unbound brain fraction ( $f_{\text{uB}}$ ) was determined in a 96-well equilibrium dialysis apparatus (HTDialysis, Gales Ferry, CT) using a previously reported method (Kalvass and Maurer, 2002). Briefly, fresh rat plasma and brain tissue were obtained the day of the study. Spectra-Por 2 membranes obtained from Spectrum Laboratories Inc. (Rancho Dominguez, CA) were conditioned in HPLC water for 15 min, followed by 30% ethanol for 15 min and 100 mM sodium phosphate pH 7.4 buffer for 15 min. Brain tissue was diluted 3-fold with 100 mM sodium phosphate (pH 7.4) buffer and homogenized with a sonic probe. Atomoxetine was added to plasma (3  $\mu\text{M}$ ) and brain tissue homogenate (1  $\mu\text{M}$ ) and 150- $\mu\text{l}$  aliquots ( $n=3$ ) were loaded into the 96-well equilibrium dialysis apparatus and dialyzed against an equal volume of 100 mM sodium phosphate (pH 7.4) buffer for 4.5 hr in a 155 rpm shaking water bath maintained at 37°C. Prior experience with the equilibrium dialysis apparatus indicated that equilibrium would be achieved by the end of the specified incubation period (data not shown). Following incubation, 10  $\mu\text{l}$

DMD#23119

of matrix (plasma and brain homogenate) and 50  $\mu$ l of buffer were removed from the apparatus and added directly to HPLC vials containing 100  $\mu$ l of an appropriate internal standard in methanol. A 50- $\mu$ l aliquot of control buffer was added to the brain homogenate and plasma samples, and 10  $\mu$ l aliquot of either control brain homogenate or control plasma was added to the buffer samples to yield identical matrix composition for all samples prior to analysis. The samples were vortex-mixed, centrifuged, and the supernatant was analyzed by the HPLC-MS/MS as described in the section Sample Collection, Preparation and Analysis. The  $f_{uP}$  was calculated from the ratio of concentrations determined in buffer versus plasma. Equation 1, which accounts for the effect of tissue dilution on unbound fraction (Kalvass and Maurer, 2002), was used to calculate  $f_{uB}$ :

$$\text{Undiluted } f_u = \frac{1/D}{((1/f_{u, \text{measured}}) - 1) + 1/D} \quad (1)$$

where D represents the fold dilution of brain tissue, and  $f_{u, \text{measured}}$  is the ratio of concentrations determined in buffer versus brain homogenate samples.

**Sample Collection, Preparation and Analysis.** Blood and dialysate samples were collected in refrigerated fraction collectors during the live phase portion of the study. Microdialysis samples were collected in a Univentor 820 microsampler (Scipro Inc., Sanborn, NY) and blood samples were collected using the Culex system (Bioanalytical Systems). Blood was collected in disodium EDTA tubes and centrifuged to generate plasma within 30 minutes of collection. Whole brain and CSF were collected from each animal at the conclusion of the live phase. Prior to collection and storage at  $-70^\circ\text{C}$ , brains

DMD#23119

were removed of atomoxetine-containing blood via carotid arterial perfusion with cold saline. The CSF was collected from the cisterna magnum. Plasma, dialysate and CSF samples were stored in a 96-well plate at  $-70^{\circ}\text{C}$  prior to analysis.

Whole brains were homogenized in acetonitrile at a ratio of 2 ml per gram of brain and centrifuged at 3,000 rpm for 10 minutes at ambient temperature using a Beckman GPR centrifuge with a GH 3.7 swinging bucket rotor. Aliquots of 50  $\mu\text{L}$  of supernatant were pipetted into a 96-well plate in duplicate for each brain. These supernatants as well as dialysate and CSF samples were analyzed for atomoxetine using standard LC-MS/MS methodology (Shimadzu HPLC with Sciex API 4000 mass spectrometer).

**Retrodialysis Calibrator Validation and Loss.**  $^2\text{H}_7$ -atomoxetine and atomoxetine are structurally similar molecules (Figure 1). Therefore, the dialyscence properties of  $^2\text{H}_7$ -atomoxetine and atomoxetine should be similar across the microdialysis probe and  $^2\text{H}_7$ -atomoxetine should suffice as a retrodialysis calibrator for atomoxetine. To confirm,  $^2\text{H}_7$ -atomoxetine and atomoxetine were prepared in dialysis buffer (100 ng/mL) and co-perfused through the microdialysis probe at a rate of 1  $\mu\text{L}/\text{min}$  over 8 hours. Dialysate was collected at 0.5 hour intervals and the mid-point of the dialysate collection period served as the dialysate collection time. The ratio of the dialysate concentrations of atomoxetine to  $^2\text{H}_7$ -atomoxetine at each collection period was assessed over time.

Dialysis buffer containing  $^2\text{H}_7$ -atomoxetine was perfused through the microdialysis probe at a rate of 1  $\mu\text{L}/\text{min}$  in PK studies. Perfusion of  $^2\text{H}_7$ -atomoxetine was initiated 4 hours prior to atomoxetine administration in the PK studies where atomoxetine was systemically infused for 4 hours; the total perfusion time of  $^2\text{H}_7$ -atomoxetine was 8 hours.

DMD#23119

In the PK studies where atomoxetine was systemically infused for 8 hours, perfusion of  $^2\text{H}_7$ -atomoxetine started at time zero (along with atomoxetine). For additional study design details see section Pharmacokinetic Study Designs. The loss (L) of  $^2\text{H}_7$ -atomoxetine across the microdialysis probe at each collection time was estimated by the loss from the perfusate during the retrodialysis period using the equation,

$$L = \frac{C_{in} - C_{out}}{C_{in}} \quad (2)$$

where  $C_{in}$  is the concentration of  $^2\text{H}_7$ -atomoxetine in the incoming perfusate (100 ng/mL) and  $C_{out}$  is the concentration of  $^2\text{H}_7$ -atomoxetine in the outgoing dialysate.

### **Pharmacokinetic Study Designs.**

*Dosing Regimens.* Three PK studies having different infusion dosing regimens were conducted. In study 1 (n=7 rats), an infusion loading dose was initially given at a rate of 10 mg/kg/h for 0.03 hours followed by an infusion maintenance dose given at a rate of 1.25 mg/kg/h for 3.97 hours. In studies 2 and 3 (n=8 rats each), an infusion loading dose was initially given at a rate of 14 mg/kg/h and 2.3 mg/kg/h, respectively, for 0.25 hours followed by an infusion maintenance dose given at a rate of 1.25 mg/kg/h for 7.75 hours. In total, atomoxetine was infused for 4 hours in study 1 and for 8 hours in study 2 and 3. The maintenance infusion rate was designed to target a steady-state plasma concentration of 250 ng/mL. In study 1, 2 and 3 the loading infusion rates were designed to approximate 0.3-, 0.6- and 3-times, respectively, the targeted steady-state plasma concentration. Time equal to zero was considered as the start time of the infusion loading dose for pharmacokinetic purposes.

DMD#23119

*Sample collections.* In all 3 studies, dialysate was collected at 0.5 hour intervals starting from the time of <sup>2</sup>H<sub>7</sub>-atomoxetine perfusion through the microdialysis probe until the end of the atomoxetine maintenance infusion. The mid-point of the dialysate collection period was used as the dialysate collection time for subsequent PK analyses and for estimation of atomoxetine microdialysis recovery. Blood samples were collected at the mid-point of the dialysate collection period. The CSF and whole brain samples were collected immediately following termination of the atomoxetine maintenance infusion and after euthanization via CO<sub>2</sub> asphyxiation.

At each dialysate collection period, the atomoxetine ECF concentration was calculated according to the equation,

$$ECF = \frac{C_{ATX,t}}{R} \quad (3)$$

where, C<sub>ATX,t</sub> is the measured concentration of atomoxetine in the dialysate at time t and R is the recovery of atomoxetine, which is assumed to be equal to the loss of the retrodialysis calibrator, <sup>2</sup>H<sub>7</sub>-atomoxetine.

**Brain Cell Concentration.** The atomoxetine concentration associated with the brain cell was calculated in each rat when appropriate according to the following equation,

$$C_{BC} = \frac{C_B \times V_B - C_{ECF} \times V_{ECF}}{V_{BC}} \quad (4)$$

where C<sub>B</sub> is the whole brain concentration following atomoxetine infusion, C<sub>ECF</sub> is the steady-state brain extracellular fluid concentration, V<sub>ECF</sub> is the brain extracellular fluid volume, V<sub>BC</sub> is the brain cell volume and V<sub>B</sub> is the total brain volume. Values for V<sub>ECF</sub>

DMD#23119

and  $V_{BC}$  were assumed to be 0.00029 and 0.00099 L, respectively (Mahar Doan and Boje, 2000). The sum of  $V_{ECF}$  and  $V_{BC}$  was assumed to be equal to  $V_B$  (Scism et al., 2000).

Details about the determination of  $C_B$  and  $C_{ECF}$  are found below in [Pharmacokinetic Analysis](#).

From equation 4,  $C_{BC}$  represents the total atomoxetine concentration associated with the brain cell. To estimate the unbound atomoxetine concentration associated with the brain cell ( $C_{uBC}$ ), the total atomoxetine concentration associated with the brain cell was multiplied by the unbound atomoxetine brain fraction as shown in the following equation,

$$C_{uBC} = C_{BC} \times f_{uB} \quad (5)$$

**Pharmacokinetic Analysis.** At each blood sampling time, the unbound atomoxetine plasma concentration was determined by multiplying the measured atomoxetine plasma concentration by  $f_{uP}$ . In study 1, the steady-state unbound atomoxetine plasma concentration ( $C_{uP}$ ) and  $C_{ECF}$  in each rat was determined by averaging the data collected from 2 – 4 hours post atomoxetine administration, and the  $C_{CSF}$  and  $C_B$  in each rat was determined at 4 hours post atomoxetine administration. In study 2 and 3, the  $C_{uP}$  and  $C_{ECF}$  in each rat was determined by averaging the data collected from 4 – 8 hours post atomoxetine administration, and the  $C_{CSF}$  and  $C_B$  in each rat was determined at 8 hours post atomoxetine administration. After obtaining these parameter values, the following ratios were calculated in each rat when data were available:  $C_B/C_P$ ,  $C_B/C_{ECF}$ ,  $C_{BC}/C_{ECF}$ ,  $C_{uBC}/C_{ECF}$ ,  $C_{ECF}/C_{uP}$  and  $C_{CSF}/C_{uP}$ .

DMD#23119

*Model Development.* Pharmacokinetic modeling was conducted using the software NONMEM version V level 1.1 with first order condition estimation (FOCE) with interaction. The PK model describing the disposition of unbound atomoxetine is illustrated in Figure 2. We developed a 4-compartment model consisting of a systemic compartment and a CNS compartment, which was further divided into the CSF, ECF and brain cell. The model can be described using a system of differential equations, as follows,

$$\frac{dA_p}{dt} = -\frac{CL}{V} A_p - \frac{Q_{BCB}}{V} A_p - \frac{Q_{BBB}}{V} A_p + \frac{Q_{BCB}}{V_{CSF}} A_{CSF} + \frac{Q_{BBB}}{V_{ECF}} A_{ECF} \quad (6)$$

$$\frac{dA_{CSF}}{dt} = -\frac{Q_{BCB}}{V_{CSF}} A_{CSF} + \frac{Q_{BCB}}{V} A_p + \frac{CL_{ECF-CSF}}{V_{ECF}} A_{ECF} \quad (7)$$

$$\frac{dA_{ECF}}{dt} = -\frac{Q_{BBB}}{V_{ECF}} A_{ECF} - \frac{CL_{ECF-BC}}{V_{ECF}} A_{ECF} - \frac{CL_{ECF-CSF}}{V_{ECF}} A_{ECF} + \frac{Q_{BBB}}{V} A_p + \frac{CL_{BC-ECF}}{V_{BC}} A_{BC} \quad (8)$$

$$\frac{dA_{BC}}{dt} = -\frac{CL_{BC-ECF}}{V_{BC}} A_{BC} + \frac{CL_{ECF-BC}}{V_{ECF}} A_{ECF} \quad (9)$$

where  $t$  represents time,  $A_p$  represents the amount of unbound atomoxetine in the plasma,  $A_{CSF}$  represents the amount of atomoxetine in CSF,  $A_{ECF}$  represents the amount of atomoxetine in the ECF and  $A_{BC}$  represents the amount of unbound atomoxetine associated with the brain cell. For unbound atomoxetine,  $CL$  represented the plasma clearance,  $Q_{BCB}$  represented the distributional clearance at the BCB,  $Q_{BBB}$  represented the distributional clearance at the BBB,  $CL_{ECF-CSF}$  represented the clearance from the ECF to the CSF,  $CL_{ECF-BC}$  represented the clearance from the ECF to the brain cell,  $CL_{BC-ECF}$

DMD#23119

represented the clearance from the brain cell to the ECF and  $V$  represented the plasma volume of distribution. Model terms  $V_{BC}$ ,  $V_{CSF}$  and  $V_{ECF}$  represented the volume of the brain cell, CSF and ECF, respectively.

Inter-individual variability in PK parameters were included in the model as described by the following equation,

$$P_{ij} = P_j \times \exp(\eta_{ij}) \quad (10)$$

where  $P_{ij}$  is the  $j^{\text{th}}$  parameter for the  $i^{\text{th}}$  individual,  $P_j$  is the typical population parameter estimate for the  $j^{\text{th}}$  parameter and  $\eta_{ij}$  is the deviation of  $P_{ij}$  from  $P_j$  in the  $j^{\text{th}}$  parameter for the  $i^{\text{th}}$  individual. For  $\eta_i$ , it is assumed that the parameter is normally distributed with a mean zero and a variance ( $\omega$ ) to be estimated.

Residual error was estimated using a proportional error model as described by the following equation,

$$C_{ik} = \text{Pred}_{ik} \times (1 + \sigma_{\text{prop}}), \quad (11)$$

where  $C_{ik}$  and  $\text{Pred}_{ik}$  are the measured and model-predicted concentration at the  $k^{\text{th}}$  sampling time in the  $i^{\text{th}}$  individual, respectively. The residual error,  $\sigma$ , is a random variable normally distributed with mean zero and estimated variance  $\sigma^2$ . The residual error describes errors arising from assay errors, sampling inaccuracies, and model misspecification.

DMD#23119

The PK parameters estimated were CL, V,  $Q_{BBB}$ ,  $Q_{BCB}$ ,  $CL_{ECF-CSF}$ ,  $CL_{ECF-BC}$ ,  $CL_{BC-ECF}$ ,  $\sigma$  and inter-rat variability of CL ( $\omega$ -CL) and V ( $\omega$ -V). Parameters fixed in the model were  $V_{CSF}$  [0.000250 L],  $V_{ECF}$  [0.000290 L] and  $V_{BC}$  [0.000990 L].

The model was developed using data obtained from 23 rats. A total of 498 concentrations were modeled, which consisted of 303, 23, 151 and 18 data points for plasma, CSF, ECF and unbound brain cell, respectively. The criteria used for the model evaluation were the fit between observed and predicted concentrations, the parameter's percent standard error of the estimate (% SEE), the randomization of weighted residual concentrations versus time between observed and predicted concentrations and the objective function.

**Statistical Analysis.** Unless otherwise indicated, all data shown are represented as the mean and standard deviation.

DMD#23119

## RESULTS

**Plasma and Brain Binding Assessment.** At 3  $\mu\text{M}$ , atomoxetine was highly bound to plasma and brain with an unbound fraction of  $0.13 \pm 0.01$  ( $n=3$ ) and  $0.013 \pm 0.0007$  ( $n=3$ ).

**Retrodialysis Calibrator Validation and Loss.** In *in vivo* brain microdialysis experiments  $^2\text{H}_7$ -atomoxetine and atomoxetine were co-perfused through the microdialysis probe and the dialysate concentrations of atomoxetine and  $^2\text{H}_7$ -atomoxetine were determined. Figure 3A illustrates the time-course of the ratio of atomoxetine to  $^2\text{H}_7$ -atomoxetine dialysate concentrations. These data demonstrate that both molecules have similar loss across the microdialysis probe because their concentration ratio is near unity. Figure 3B shows that  $^2\text{H}_7$ -atomoxetine loss was reproducible and from approximately 4 – 8 hours post-perfusion no discernable decrease in  $^2\text{H}_7$ -atomoxetine loss was noted. Under analogous conditions *in vitro*, a similar loss profile was observed for  $^2\text{H}_7$ -atomoxetine; furthermore,  $^2\text{H}_7$ -atomoxetine loss and gain were similar from 4 – 8 hours (data not shown). It is possible that the initial decline in  $^2\text{H}_7$ -atomoxetine loss through the initial 4 hours, either *in vitro* or *in vivo*, reflects slow equilibration of  $^2\text{H}_7$ -atomoxetine binding to the probe. Taken together, these data indicate that  $^2\text{H}_7$ -atomoxetine is a suitable retrodialysis calibrator for atomoxetine.

**Pharmacokinetics.** Figure 4 is a scatter plot of the atomoxetine plasma, CSF, ECF and whole brain concentrations across all dosing regimens. The steady-state plasma, CSF, ECF and whole brain concentrations were  $268 \pm 98$  ( $n=25$ ),  $43 \pm 14$  ( $n=26$ ),  $17 \pm 11$  ( $n=18$ ) and  $2790 \pm 809$  ( $n=26$ ), respectively. The atomoxetine steady-state concentration ratios were calculated. The  $C_B/C_P$  and  $C_B/C_{ECF}$  values were determined to be  $11 \pm 3$  ( $n=25$ ) and  $170 \pm 60$  ( $n=18$ ), respectively, and the  $C_{ECF}/C_{uP}$  and  $C_{CSF}/C_{uP}$  values were  $0.7 \pm 0.4$  ( $n=18$ )

DMD#23119

and  $1.7 \pm 0.8$  ( $n=25$ ), respectively. The  $C_{BC}/C_{ECF}$  and  $C_{uBC}/C_{ECF}$  values were  $219 \pm 77$  ( $n=18$ ) and  $2.9 \pm 1.0$  ( $n=22$ ), respectively. A 4-compartment semi-physiological model comprised of a systemic compartment and a CNS compartment, which was further divided into the CSF, ECF and brain cell, was used to obtain PK parameter estimates unbound atomoxetine (see Figure 2). The PK parameters estimated from the model are shown in Table 1. The data supported estimation of all model parameters with acceptable precision. The model population and individual predicted concentrations versus measured concentrations were close to the line of unity indicating an acceptable fit of the data to the model (Figure 5). Taken together, these data indicate that the model adequately characterizes the disposition of unbound atomoxetine.

DMD#23119

## DISCUSSION

The ability to cross the BBB and BCB is important for drugs with targets in the CNS. It is a commonly accepted assumption that unbound drug is the entity available for interaction with drug targets and is referred to as the free drug hypothesis. It is also assumed that unbound drug in brain is in direct contact or in equilibrium with the site of action (de Lange and Danhof, 2002). For a compound that distributes solely by passive diffusion, at distribution equilibrium the unbound concentration in brain ( $C_{uB}$ ) will equal the unbound concentration in plasma ( $C_{uP}$ ) and the expected steady-state brain partition coefficient ( $K_{p,exp}$ ) can be described using these estimates ( $K_{p,exp} = f_{uP}/f_{uB}$ ). We determined  $f_{uP}$  and  $f_{uB}$  to be 0.131 and 0.013, respectively, ( $K_{p,exp} = 10$ ), consistent with previous literature estimates (Mattiuz et al. 2003; Summerfield et al., 2007). This value of  $K_{p,exp}$  was similar to the observed steady-state brain partition coefficient ( $K_{p,obs}$ ) following intravenous infusion of atomoxetine obtained in this study, where  $K_{p,obs} = C_B/C_P = 11$ . These data further support the work of Kalvass and Maurer (2002) and the utility of predicting  $K_{p,obs}$  from  $K_{p,exp}$  for drugs in which BBB transport is primarily passive ( $K_{p,exp}/K_{p,obs} \approx 1$ ). Based on brain microdialysis, we determined the steady-state  $C_{ECF}/C_{uP}$  to be 0.7 and near unity. In total, these two sets of data obtained by distinct methodologies are in accordance and are consistent with the transport of atomoxetine across the BBB being primarily passive.

Based on  $C_B/C_{ECF}$  and  $C_{BC}/C_{ECF}$  ratios of 170 and 219, respectively, we conclude that whole brain concentrations of atomoxetine do not represent the concentration of drug in the biophase and partitioning of atomoxetine within brain cells is substantial. We acknowledge that the calculation of the steady-state  $C_{BC}$  (equation 4) does not

DMD#23119

differentiate between bound or unbound atomoxetine in the cell, and therefore, limits an understanding of the mechanism of the partitioning. We used our estimate of  $f_{uB}$  to calculate the steady-state  $C_{uBC}$ . To do this, we assumed that the brain tissue homogenization process and disruption of the tissue membranes did not compromise the value of  $f_{uB}$  and that this value accurately reflects in vivo binding. We also make the distinction that  $f_{uB}$  is a function of intracellular and/or cell membrane binding only. The  $C_{uBC}/C_{ECF}$  was determined to be 2.9 and substantially less than  $C_{BC}/C_{ECF}$  ( $\approx 219$ ) showing that atomoxetine does not preferentially reside in the extracellular space. We adopted the concept of others (Kalvass et al., 2007; Maurer et al., 2005) based on  $C_{uBC}/C_{ECF}$  within 3-fold of unity to suggest that atomoxetine passively distributes within brain parenchyma. Friden et al. (2006) demonstrated an inherent inability of the brain homogenization technique to predict  $K_{p,obs}$  for drugs that preferentially reside in the extracellular space in vivo. Consistent with our results for atomoxetine, the brain homogenization technique and brain microdialysis were in accordance.

We determined  $C_{CSF}/C_{uP}$  to be 1.7, and like the BBB, conclude that the transport of atomoxetine is primarily passive across the BCB. The concept of a sink action of CSF suggests that the  $C_{CSF}/C_{ECF}$  value of a drug that undergoes only passive diffusion across the BBB and BCB should be below unity. The atomoxetine  $C_{CSF}/C_{ECF}$  ratio was determined to be 3, which is not considered to be meaningfully different from unity. Given the extensive partitioning of atomoxetine in brain tissue, this finding indicates that CSF bulk flow is not a significant determinant of atomoxetine residence time in the CSF. We developed a neuropharmacokinetic model accordingly by incorporating a distributional clearance parameter at the BBB ( $Q_{BBB}$ ) and at the BCB ( $Q_{BCB}$ ). We

DMD#23119

explored estimation of bi-directional clearances at both the BBB and BCB but found that model parameters were estimated more precisely when distributional clearances at the BBB and BCB were contained in the model. The values of  $Q_{BBB}$  and  $Q_{BCB}$  were estimated to be 0.00110 L/h and 0.0000909 L/h. The  $Q_{BBB}/Q_{BCB}$  ratio was about 12 indicating the distributional clearance across the BBB was more rapid than the distributional clearance across the BCB, consistent with the larger surface area of the BBB relative to the BCB. Although definitive data are lacking, there appears to be a favored movement of drug from ECF to CSF, rather than the reverse (Rosenberg et al., 1980; Shen et al., 2004). Therefore, in our model, CSF concentrations of atomoxetine are due to direct availability from passage across the BCB or indirectly by passage across the BBB followed by diffusion or convective flow from the ECF. Our model characterized the unidirectional transport from ECF to CSF ( $CL_{ECF-CSF}$ ). In rats, the first-order rate constant for flow from ECF to CSF ( $k_{ECF-CSF}$ ) and  $V_{ECF}$  were estimated to be  $0.084 \text{ h}^{-1}$  and 0.00029 L, respectively (Szentistvanyi et al., 1984). Taken together, a theoretical value for  $CL_{ECF-CSF}$  is proposed to be 0.000024 L/h ( $CL_{ECF-CSF} = k_{ECF-CSF} \times V_{ECF}$ ). During model development,  $CL_{ECF-CSF}$  was either fixed to the theoretical value or estimated. When estimated,  $CL_{ECF-CSF}$  was 0.000129 L/h and approximately 5-times larger than the theoretical value. The cause for this difference is not known. An investigation of the metabolism of atomoxetine in brain may provide insight for this result. Importantly, estimating  $CL_{ECF-CSF}$  provided a better fit of the data to the model (data not shown).

The transport across brain parenchyma was modeled using bi-directional clearances where  $CL_{ECF-BC}$  represented the clearance from ECF to brain cell and  $CL_{BC-ECF}$

DMD#23119

represented the clearance from brain cell to ECF. We attempted to estimate a distributional clearance at this site but found that the model parameters were not estimable when doing so. The values of  $CL_{ECF-BC}$  and  $CL_{BC-ECF}$  were estimated to be 0.00216 L/h and 0.000934 L/h, respectively. The  $CL_{ECF-BC}/CL_{BC-ECF}$  ratio was 2.3, and as anticipated, consistent with our calculation of  $C_{uBC}/C_{ECF}$  ( $\approx 2.9$ ).

In summary, we have carried out the first detailed examination using a quantitative microdialysis technique to understand the brain disposition of atomoxetine, a centrally-acting NET inhibitor used for the clinical treatment of ADHD. We found that atomoxetine is highly bound to brain tissue and that total brain atomoxetine concentration is not reflective of the concentration in brain ECF, the site where atomoxetine acts to inhibit NE re-uptake into the neuron. Data obtained from this study suggest that atomoxetine brain penetration is high, movement of atomoxetine across the BBB and BCB occur predominantly by a passive mechanism and rapid equilibration of ECF and CSF with plasma occurs. In addition, we developed a model to describe the neuropharmacokinetic behavior of atomoxetine, which enhances our understanding of this molecule as a therapeutic entity.

**Acknowledgements.** Jennifer Hanes for her microdialysis technical expertise, Justus Enoch Bingham for his pharmacokinetic analysis support, Siak Leng Choi and Lisa Ferguson-Sells for their documentation quality review and Michael Harris for his bioanalytical support.

DMD#23119

## REFERENCES

- Biederman J (2005) Attention-deficit/hyperactivity disorder: a selective overview. *Biol Psychiatry* **57(11)**:1215-1220.
- Biederman J and Faraone SV (2002) Current concepts on the neurobiology of attention-deficit/hyperactivity disorder. *J Atten Disord* **6 (Suppl. 1)**: S7-S16.
- Bymaster FP, Katner JS, Nelson DL, Hemrick-Luecke, SK, Threlkeld PG, Heiligenstein JH, Morin SM, Gehlert DR, Perry KW (2002) Atomoxetine increases extracellular levels of norepinephrine and dopamine in prefrontal cortex of rat: a potential mechanism for efficacy in attention deficit/hyperactivity disorder. *Neuropsychopharmacology* **27(5)**: 699-711.
- de Lange EC and Danhof M (2002) Considerations in the use of cerebrospinal fluid pharmacokinetics to predict brain target concentrations in the clinical setting: implications of the barriers between blood and brain. *Clin Pharmacokinet* **41(10)**: 691-703.
- Doran A, Obach RS, Smith BJ, Hosea NA, Becker S, Callegari E, Chen C, Chen X, Choo E, Cianfrogna J, Cox LM, Gibbs JP, Gibbs MA, Hatch H, Hop CE, Kasman IN, Laperle J, Liu J, Liu X, Logman M, Maclin D, Nedza FM, Nelson F, Olson E, Rahematpura S, Raunig D, Rogers S, Schmidt K, Spracklin DK, Szewc M, Troutman M, Tseng E, Tu M, Van Deusen JW, Venkatakrishnan K, Walens G, Wang EQ,

DMD#23119

Wong D, Yasgar AS, Zhang C (2005) The impact of P-glycoprotein on the disposition of drugs targeted for indications of the central nervous system: evaluation using the MDR1A/1B knockout mouse model. *Drug Metab Dispos* **33(1)**: 165-74

Fridén M, Gupta A, Antonsson M, Bredberg U, Hammarlund-Udenaes M (2007) In vitro methods for estimating unbound drug concentrations in the brain interstitial and intracellular fluids. *Drug Metab Dispos* **35(9)**: 1711-9.

Kalvass JC, Maurer TS, Pollack GM (2007) Use of plasma and brain unbound fractions to assess the extent of brain distribution of 34 drugs: comparison of unbound concentration ratios to in vivo p-glycoprotein efflux ratios. *Drug Metab Dispos* **35(4)**: 660-6

Kalvass JC and Maurer TS (2002) Influence of nonspecific brain and plasma binding on CNS exposure: implications for rational drug discovery. *Biopharm Drug Dispos* **23(8)**: 327-38

Mahar Doan KM and Boje KM (2000) Theoretical pharmacokinetic and pharmacodynamic simulations of drug delivery mediated by blood--brain barrier transporters. *Biopharm Drug Dispos* **21(7)**: 261-78

Mattiuz EL, Ponsler GD, Barbuch RJ, Wood PG, Mullen JH, Shugert RL, Li Q, Wheeler WJ, Kuo F, Conrad PC, Sauer JM (2003) Disposition and metabolic fate of

DMD#23119

atomoxetine hydrochloride: pharmacokinetics, metabolism, and excretion in the Fischer 344 rat and beagle dog. *Drug Metab Dispos* **31(1)**: 88-97

Maurer TS, Debartolo DB, Tess DA, Scott DO (2005) Relationship between exposure and nonspecific binding of thirty-three central nervous system drugs in mice. *Drug Metab Dispos* **33(1)**: 175-81

Rosenberg GA, Kyner WT, Estrada E (1980) Bulk flow of brain interstitial fluid under normal and hyperosmolar conditions. *Am J Physiol Ren Physiol* **238(1)**: F42-49.

Sauer JM, Ponsler GD, Mattiuz EL, Long AJ, Witcher JW, Thomasson HR, Desante KA (2003) Disposition and metabolic fate of atomoxetine hydrochloride: the role of CYP2D6 in human disposition and metabolism. *Drug Metab Dispos* **31(1)**: 98-107.

Scism JL, Powers KM, Artru AA, Lewis L, Shen DD (2000) Probenecid-inhibitable efflux transport of valproic acid in the brain parenchymal cells of rabbits: a microdialysis study. *Brain Res* **884**: 77-86.

Shen DD, Artru AA, Adkison KK (2004) Principles and applicability of CSF sampling for the assessment of CNS drug delivery and pharmacodynamics. *Adv Drug Deliv Rev* **56(12)**:1825-57.

DMD#23119

Summerfield SG, Read K, Begley DJ, Obradovic T, Hidalgo IJ, Coggon S, Lewis AV, Porter RA, Jeffrey P (2007) Central nervous system drug disposition: the relationship between in situ brain permeability and brain free fraction. *J Pharmacol Exp Ther* 322(1):205-13.

Szentistványi I, Patlak CS, Ellis RA, Cserr HF (1984) Drainage of interstitial fluid from different regions of rat brain. *Am J Physiol Ren Physiol* 246:F835-44.

DMD#23119

## FOOTNOTES

Reprint requests should be sent to:

Dr. William Kielbasa

Lilly Research Laboratories

Eli Lilly and Company

Indianapolis, IN 46285

e-mail: [kielbasa\\_william@lilly.com](mailto:kielbasa_william@lilly.com)

DMD#23119

## FIGURE LEGENDS

Figure 1. Structures of Atomoxetine and the Retrodialysis Calibrator  $^2\text{H}_7$ -Atomoxetine

Figure 2. Schematic of the Atomoxetine Neuropharmacokinetic Model

Figure 3. Dialysate Concentration Ratio of Atomoxetine and  $^2\text{H}_7$ -Atomoxetine Following Co-Perfusion Through the Microdialysis Probe (A; n=4) and Loss of  $^2\text{H}_7$ -Atomoxetine Following Perfusion Through the Microdialysis Probe (B; n=14). Data are presented as mean  $\pm$  standard deviation.

Figure 4. Individual Rat Atomoxetine Concentrations in Plasma, CSF, ECF and Whole Brain During an Intravenous Maintenance Infusion of Atomoxetine at 1.25 mg/kg/h.

Figure 5. Individual PK Model Predicted Atomoxetine Concentrations Versus Observed Atomoxetine Concentrations.

DMD#23119

## TABLES

Table I. Model Estimated Pharmacokinetic Parameters of Atomoxetine

<b>Parameter</b>	<b>Estimate (%SEE)</b>	<b>Inter-rat Variability (%SEE)</b>
CL (L/h)	14.5 (8.69)	38.6 (23.7)
V (L)	6.92 (30.8)	65.4 (80.1)
Q <sub>BCB</sub> (L/h)	0.0000909 (29.9)	---
Q <sub>BBB</sub> (L/h)	0.00110 (34.5)	---
CL <sub>ECF-CSF</sub> (L/h)	0.000129 (20.2)	---
CL <sub>ECF-BC</sub> (L/h)	0.00216 (25.1)	---
CL <sub>BC-ECF</sub> (L/h)	0.000934 (25.7)	---
V <sub>BC</sub> (L)	0.000990 (fixed)	---
V <sub>CSF</sub> (L)	0.000250 (fixed)	---
V <sub>ECF</sub> (L)	0.000290 (fixed)	---
$\sigma_{prop}$	34.7 (9.09)	---

Abbreviations: CL, unbound plasma clearance; Q<sub>BCB</sub>, distributional clearance at the BCB; Q<sub>BBB</sub>, distributional clearance at the BBB; CL<sub>ECF-CSF</sub>, clearance from the ECF to the CSF; CL<sub>ECF-BC</sub>, clearance from the ECF to the brain cell; CL<sub>BC-ECF</sub>, clearance from the brain cell to the ECF; V, unbound plasma volume of distribution; V<sub>BC</sub>, brain cell volume; V<sub>CSF</sub>, CSF volume; V<sub>ECF</sub>, brain ECF volume;  $\omega$ , inter-animal variability;  $\sigma_{prop}$ , proportional residual error; %SEE, percent standard error of the estimate; CV, coefficient of variation.

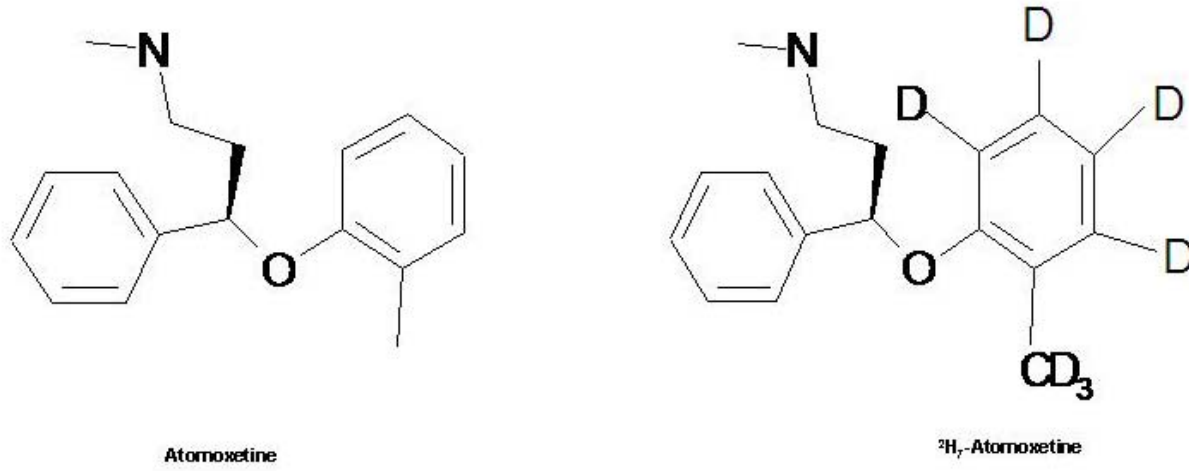
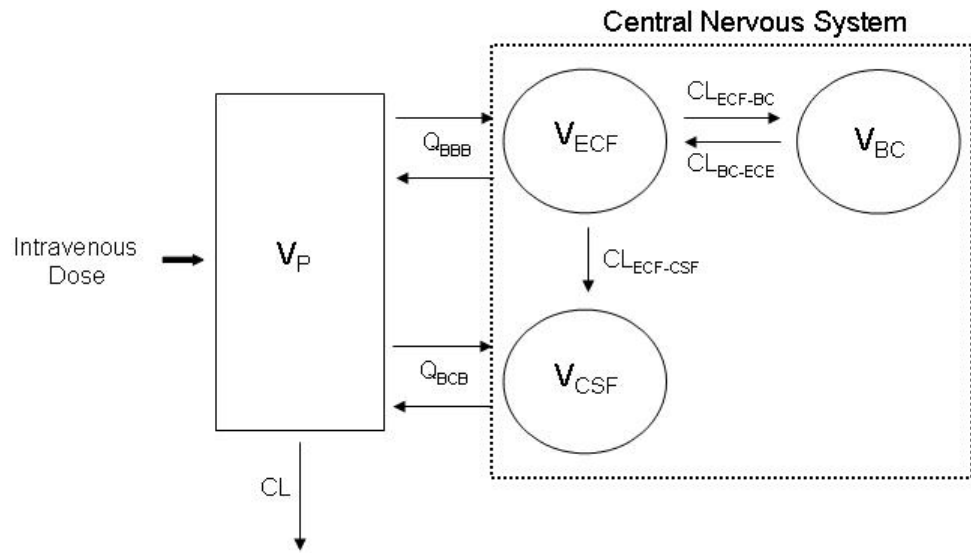


Figure 1



**Figure 2**

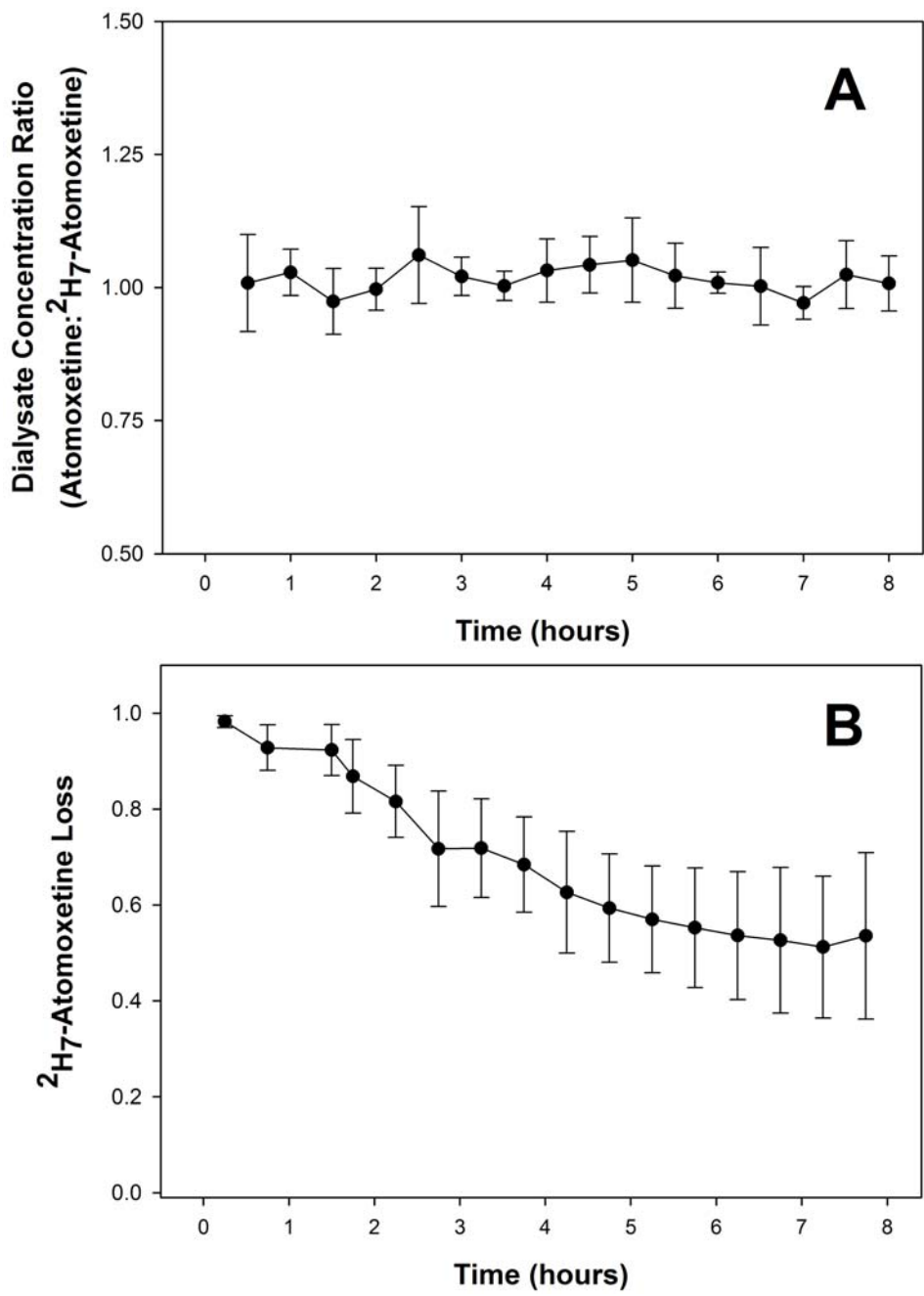


Figure 3

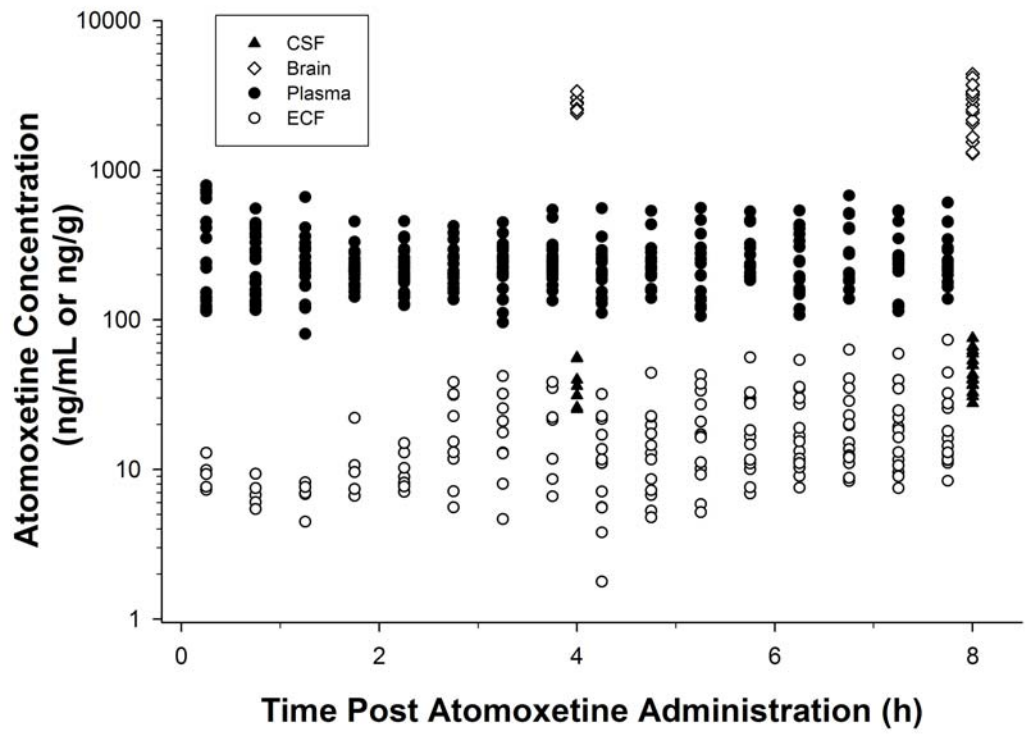


Figure 4

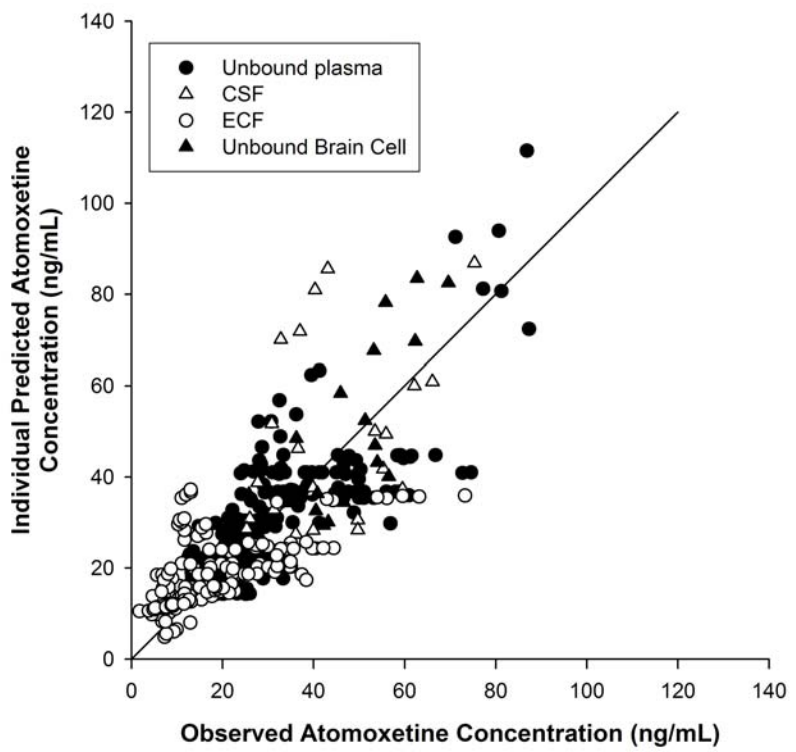


Figure 5